2021 IEEE 18th International Symposium on Biomedical Imaging (ISBI)
April 13-16, 2021, Nice, France

2021 IEEE 18th International Symposium on Biomedical Imaging (ISBI) | 978-1-6654-1246-9/20/$31.00 ©2021 IEEE | DOI: 10.1109/ISBI48211.2021.9433867

TOPOLOGY PRESERVING SEGMENTATION FUSION FOR CELLS WITH COMPLEX SHAPES

Aleksandra Melnikova, Petr Matula

Masaryk University, Faculty of Informatics
Centre for Biomedical Image Analysis
Brno, Czech Republic

ABSTRACT

We present an algorithm to fuse simply connected segmentation masks of complex and variable shapes that often appear in cell imaging. The algorithm is designed to preserve topology of the input masks and to faithfully represent their protrusions. It works in three main phases: (1) the detection of geodesic ends that correspond to the protrusions, (2) optimal matching of the geodesic ends, and (3) contour averaging of corresponding boundary segments. We show that our algorithm overcomes commonly used pixel-wise fusion algorithms (namely majority voting, SIMPLE, STAPLE, and topology-preserving STAPLE), as well as recently published geometric median shapes in terms of the visual quality of results as well as better representation of protrusions. We demonstrate the performance of our method based on synthetic images as well as real images from the cell segmentation benchmark datasets.

Index Terms— Segmentation fusion, Reference annotation, Cell annotation, Shape

1. INTRODUCTION

The evaluation of image segmentation algorithms requires reference annotations. Because the exact reference annotation (ground-truth) is rarely known and often even impossible to obtain, a common strategy is to construct so-called gold truth by fusing several human annotations, see e.g., [1–6]. The general idea is to take either segmentation masks (i.e., the set of points that belong to the object) or object contours (i.e., the set of points that form the object boundary) and to create a fused segmentation mask or fused object contour that is used to evaluate the segmentation algorithms.

As the image segmentation problem is often formulated as a classification problem on the pixel level, a large number of annotation fusion algorithms work pixel-wise by combining labels of each pixel. A good example from this category is the majority-voting scheme (MV) [2, 3], which is a simple, effective, and probably the most straightforward way for the annotation fusion used in practice (e.g., used in [7]). Other well-known pixel-based methods are SIMPLE [6] and STAPLE [4]. The STAPLE algorithm is an expectation maximization algorithm that computes a probabilistic estimation of segmentation annotation fusion. A topology-preserving version of STAPLE (we denote it as T-STAPLE) can be acquired by adding topology-correction step [8]. The SIMPLE is an iterative algorithm that combines the label selection and performance estimation strategies. Such an approach allows to take into account only labels that are considered as reliable. It was shown that SIMPLE could serve as an alternative to STAPLE for combining expert-made reference segmentations [6]. Other label fusion methods based on level-sets, LSML, and its variant with shape priors LSMLP, were proposed in [5]. The LSMLP approach allows to incorporate the shape priors by computing the additional MV image and adding it to the energy function. A comparison of MV, STAPLE, SIMPLE and LSML algorithms was presented in [9]. The authors concluded that STAPLE and LSML algorithms can compute a balanced annotation when the variance within the annotation set is low. However, the performance of different fusion algorithms depends on the dataset, the level of agreement within annotations and the metric that is used for comparison. As the pixel-wise algorithms do not treat the object masks as a whole, they do not, in general, guarantee to preserve topology of the initial annotations and can introduce weird results at the object boundaries (see, e.g., the first four leftmost columns in Fig. 3 and compare them with the individual annotations in Fig. 1, columns A1, A2, and A3).

Another possibility to obtain a reference annotation is to calculate an average shape out of the set of input shapes, where shapes, in this paper, are understood as closed object contours [10]. Because the shapes are pre-aligned as we combine the annotations of the same image, the problem is simpler than, for example, in statistical shape modelling or building anatomical atlases where typically an average shape over a set of different subjects is needed. On the other hand, in the main intended application of our method, which is cell imaging, the cells can have highly variable and complex shapes

The work was founded by the Czech Science Foundation, project no. GA21-20374S.

that can contain many protrusions and it is important to recover the cell shapes as best as possible because they are related to the cell function and therefore important in cell studies [11, 12]. Especially if the protrusions are thin, it is difficult for human annotators to draw them at the same place and therefore they can easily be removed from the data by averaging. This difficulty can be observed in the results of the geometrical median shapes (GEMS) [13], which is a recently published state-of-the-art shape averaging method included into our comparisons (see the second right column in Fig. 3 and compare it with the individual annotations in Fig. 1).

In this paper, we propose an algorithm to fuse segmentation masks of complex and variable shapes that often appear in cell imaging designed to preserve the topology of the initial annotations under the condition the masks are simply connected sets (Section 2). As the main contribution, we present that our algorithm overcomes the state-of-the-art and popular segmentation fusion algorithms (namely MV, SIMPLE, STAPLE, T-STAPLE, and GEMS) in terms of its ability to faithfully represent complex cell shapes with protrusions in the data (Section 3 and 4).

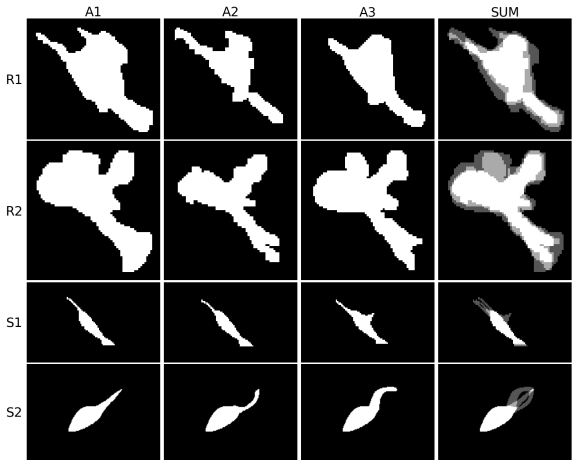

Fig. 1. Example of real (from the cell segmentation benchmark datasets, rows R1 and R2) and synthetic data (rows S1 and S2). The synthetic data were created for the demonstration of the performance of fusion algorithms.

2. METHOD DESCRIPTION

The proposed method fuses a set of segmentation masks, which are assumed to be simply connected objects, into one in the following three main steps: (1) a detection of geodesic ends that correspond to object protrusions, (2) the geodesic end matching combined with a selection of corresponding boundary segments, and (3) averaging of the corresponding boundary segments. The detection of geodesic ends is performed as a local maximum search on the object boundaries where each boundary point has assigned the longest geodesic distance over all points in the mask. The matching between the geodesic ends for each pair of input masks is formulated as an optimal assignment problem and efficiently solved by the Hungarian algorithm. For calculating the final mask, we average the contour segments of corresponding geodesic ends by a spline interpolation and fill the obtained closed curve to get a simply connected object in order to preserve the topology of the inputs (See Fig. 2).

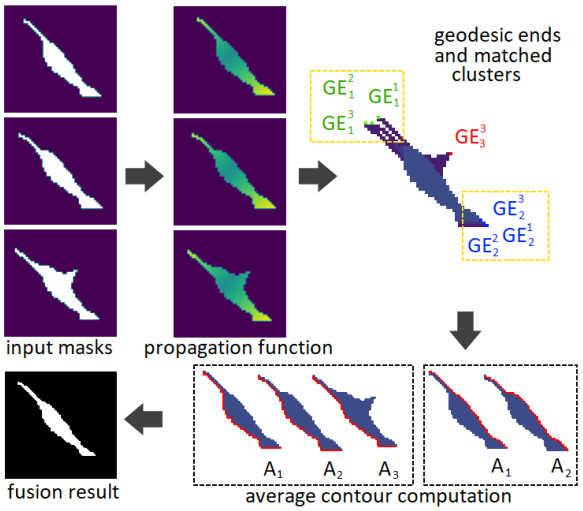

Fig. 2. The scheme of the proposed algorithm.

More formally, the algorithm takes N annotations (simply connected segmentation masks) as an input. We define the propagation function P at a given pixel x of a set X to be [14]:

$$P_X(x) = \max\{d_X(x,y) \,|\, y \in X\}, \forall x \in X, \qquad (1)$$

where $d_X(x,y)$ is the geodesic distance between x and y within the set X. The *geodesic distance* between two points is defined as the minimum length of the path inside the set connecting the two points. *Geodesic ends* of X are the regional maxima of its propagation function.

Step 1: Let $A_1, A_2, \ldots, A_N$ be the input annotations. For each annotation A_i, we compute the propagation function (Eq. 1) and find geodesic ends $GE^i = \{GE^i_k\}$, $k = 1, \ldots, M_i$ (M_i is the number of geodesic ends in mask A_i). We can compute the propagation function only on the object boundaries, for efficiency.

Step 2: Having found the geodesic ends, we match them for each pair of input annotations A_i and A_j. We used the Hungarian (also known as Kuhn-Munkres) algorithm for the matching similarly as in [15]. We use the matrix formulation of the problem. We define the cost matrix B_{ij} of size $(M_i + M_j) \times (M_i + M_j)$ with elements $(B_{ij})_{kl} = d_{max} - d_e(GE^i_k, GE^j_l)$ for all $k \leq M_i$ and $l \leq M_j$, and set $(B_{ij})_{kl} = 0$ otherwise; d_e is the Euclidean distance and d_{max} is the threshold (maximum allowed displacement of geodesic ends). If two GEs are further then

d_{max} they can not be matched. Having the cost matrix composed, we can perform matching for GEs by Kuhn-Munkres algorithm for each pair of A_i, A_j. The employment of the Euclidean distance is justified by the problem statement: annotations are typically very similar and reasonably well aligned as the experts annotate the same objects. However, additional features such as orientation or geodesic length could be included into the cost computation if necessary, e.g., in datasets with many close protrusions.

The result of the matching step is a list of matched GEs. We can consider this list as a graph with vertices $V = \bigcup_{i=1}^{N} GE^i$ and edges E given by the matching. We search for the connected components (CC) in the graph (V, E), which corresponds to clusters of matched points. As a result, GEs without correspondences are excluded (V_{excl}), which provides robustness to outliers in the annotation set (CC are denoted by yellow dashed lines in Fig. 2).

Step 3: Let us call CC_m and CC_n adjacent if there exist $GE^i_k \in CC_m, GE^i_l \in CC_n$ for some annotation A_i such that they can be connected by a segment $\gamma(GE^i_k, GE^i_l)$ of the contour (boundary) of A_i and there are no other GE from $V \backslash V_{excl}$ lying on this segment. Denote by P_{mn} be the set of all such pairs (GE^i_k, GE^i_l). For each pair CC_m, CC_n of adjacent CCs we compute the mean γ_{mn} over $\{\gamma(p) \,|\, p \in P_{mn}\}$.To avoid discretization problems we use spline interpolation.

Finally, we construct resulting contour Γ by concatenating the averaged segments γ_{mn}. Because we calculate centroids of all endpoints in CCs the concatenation of the average segments must return a closed curve. The final mask can be obtained by filling the contour. As the resulting contour is closed by construction, the obtained mask must be simply connected as all the initial annotations.

Pseudo code of the proposed algorithm is presented in Algorithm 1.

Algorithm 1: The proposed fusion algorithm

Input: $A_1, A_2, ...A_N$ // masks of individual annotations
Output: A // final segmentation mask
$\Gamma = \emptyset$ // set of contour points (initially empty)
for *i= 1* **to** *N* **do**
  GE^i = `computeGeodesicEnds`(A_i) // list of GEs
  $M_i = |GE^i|$
end
foreach $(i, j) \in \{1, ..., N\} \times \{1, ..., N\}$ **do**
  B_{ij} = `costMatrix`$(GE^i, GE^j) \in \mathbb{R}^{(M_i+M_j)\times(M_i+M_j)}$
  E_{ij} = `hungarianAlgorithm`(B_{ij})
  // compute matching between GEs
end
$V = \bigcup_{i=1}^{N} GE^i$, $E = \bigcup_{i,j=1}^{N} E_{ij}$
$\{CC\}$ = `findCC`(V, E) // find connected components
foreach $(CC_m, CC_n) \in$ `adjacent`$(\{CC\})$ **do**
  // loop over all pairs of connected GEs
  foreach $p \in P_{mn}$ **do**
    $\gamma(p)$ = `spline`(p) // interpolate the segment between connected GEs
  end
  γ_{mn} = `average`$(\{\gamma(p) \,|\, p \in P_{mn}\})$
end
Γ = `concatenate`$(\{\gamma_{mn}\})$
A = `fill`(Γ)
return A

3. EXPERIMENTAL RESULTS

We compared the proposed method with the following commonly used pixel-wise fusion algorithms: MV, SIMPLE, STAPLE, and T-STAPLE, and a recently published contour-based algorithm GEMS. We applied these algorithms to synthetic as well as real masks (see Fig. 1 for representative examples). The real data were taken from the cell segmentation benchmark datasets [7]. The synthetic images were prepared to demonstrate the limitations of the compared fusion methods.

By design, the proposed algorithm preserves topology of the input segmentation masks. All inputs are simply connected objects and the output mask must also have this property, as described above (see Fig. 1 and Fig. 3 for illustration). The proposed algorithm correctly reconstructs the thin details and recovers them better than any other algorithm included in the comparison. This property comes from the matching step of the geodesic ends, which ensures, that the thin protrusions are correctly represented. The presented examples of experiments on the real data demonstrate that pixel-wise fusion methods might result in border artifacts, while GEMS and the proposed method obtain a smother border without artifacts (see Fig. 3). Also, GEMS and T-STAPLE preserve topology of the data. However, as can be seen on the synthetic data, GEMS and T-STAPLE still fail to preserve certain thin details when they are displaced in the input annotations. Our method can reconstruct thin protrusions well even when they are shifted. Finally, our method is robust to outliers (Fig. 3) as only the geodesic ends with correspondences are involved in the computation of the average contour (see Step 2 in Section 2, row S1 in Fig. 1 and Fig. 3, where the small protrusion that appears in A3 only is ignored in the final result.).

4. CONCLUSION

We presented a novel label fusion algorithm that preserves the topology of the initial annotations, which is robust to outliers and shifts of thin protrusions. The experiments show that commonly used pixel-wise methods (MV, SIMPLE, STAPLE, and T-STAPLE) can produce artifacts on the border and do not preserve topology (except for T-STAPLE). The GEMS method represents the shapes better than the compared pixel-wise methods, but it has difficulties to recover thin protrusions. The proposed method was the only one that could recover them well. The obtained results suggest the

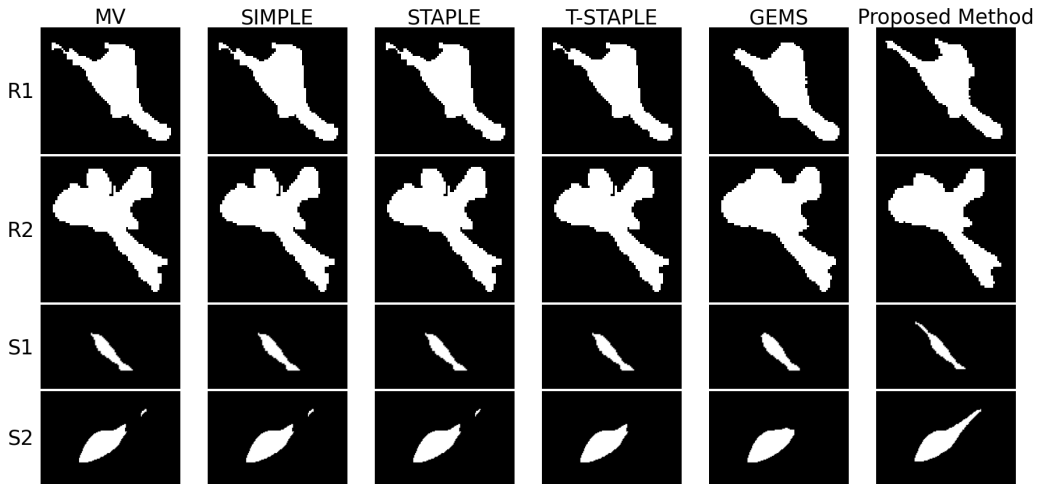

Fig. 3. Examples of experiments on real (rows R1 and R2) and synthetic data (rows S1 and S2): fusion of three annotations (Fig. 1), from left to right: MV, SIMPLE, STAPLE, T-STAPLE, GEMS and the proposed method.

method to be applicable for fusing reference annotations of cells with complex shapes.

5. REFERENCES

[1] C. Emre Akbas et al., "Automatic fusion of segmentation and tracking labels," in *Proceedings of the European Conference on Computer Vision (ECCV)*, 2018.

[2] X. Artaechevarria, A. Munoz-Barrutia, and C. Ortiz-de Solórzano, "Combination strategies in multi-atlas image segmentation: application to brain MR data," *IEEE transactions on medical imaging*, vol. 28, no. 8, pp. 1266–1277, 2009.

[3] J. Kittler et al., "On combining classifiers," *IEEE transactions on pattern analysis and machine intelligence*, vol. 20, no. 3, pp. 226–239, 1998.

[4] S.K. Warfield, K.H. Zou, and W.M. Wells, "Simultaneous truth and performance level estimation (STAPLE): an algorithm for the validation of image segmentation," *IEEE transactions on medical imaging*, vol. 23, no. 7, pp. 903–921, 2004.

[5] X. Li et al., "Estimating the ground truth from multiple individual segmentations incorporating prior pattern analysis with application to skin lesion segmentation," in *2011 IEEE International Symposium on Biomedical Imaging: From Nano to Macro*. IEEE, 2011, pp. 1438–1441.

[6] T.R. Langerak et al., "Label fusion in atlas-based segmentation using a selective and iterative method for performance level estimation (SIMPLE)," *IEEE transactions on medical imaging*, vol. 29, no. 12, pp. 2000–2008, 2010.

[7] V. Ulman et al., "An objective comparison of cell-tracking algorithms," *Nature methods*, vol. 14, no. 12, pp. 1141, 2017.

[8] J.A. Bogovic, P.L. Bazin, and J.L. Prince, "Topology-preserving STAPLE," in *2010 IEEE Computer Society Conference on Computer Vision and Pattern Recognition-Workshops*. IEEE, 2010, pp. 1–6.

[9] T.A. Lampert, A. Stumpf, and P. Gançarski, "An empirical study into annotator agreement, ground truth estimation, and algorithm evaluation," *IEEE Transactions on Image Processing*, vol. 25, no. 6, pp. 2557–2572, 2016.

[10] L. da Fona Costa and R.M. Cesar Jr, *Shape classification and analysis: theory and practice*, CRC Press, 2018.

[11] D.L. Bodor et al., "Of cell shapes and motion: The physical basis of animal cell migration," *Developmental Cell*, vol. 52, no. 5, pp. 550–562, 2020.

[12] A. Haupt and N. Minc, "How cells sense their own shape–mechanisms to probe cell geometry and their implications in cellular organization and function," *Journal of cell science*, vol. 131, no. 6, 2018.

[13] A. Cunha, "GEMS-geometric median shapes," in *2019 IEEE 16th International Symposium on Biomedical Imaging (ISBI 2019)*. IEEE, 2019, pp. 1492–1496.

[14] P. Soille, *Morphological image analysis: principles and applications*, Springer Science & Business Media, 2013.

[15] P. Matula et al., "Fast point-based 3-D alignment of live cells," *IEEE Transactions on Image Processing*, vol. 15, no. 8, pp. 2388–2396, 2006.